Chapter 6 Failure Predictions

Utilizing the approaches for computing the inplane and interlaminar shear stresses discussed in the previous chapter, this chapter will present a discussion of failure of internally pressurized elliptical cylinders. The Hashin and maximum stress failure criteria and geometrically linear and nonlinear analyses will be considered to predict the location and mode of failure.

6.1 Failure Predictions for the Geometrically Linear Theory

The Hashin and maximum stress failure criteria were implemented in a FORTRAN code using the stresses obtained for the geometrically linear analysis. The FORTRAN code computed the stresses in the principal material coordinate system at an internal pressure of 100 psi, then combined them as prescribed in eqs. 5.5-5.7 for the maximum stress criterion and eqs. 5.12-5.15 for the Hashin criterion. For the maximum stress criterion, the seven left-hand sides in the criterion were then computed as a function of axial, circumferential, and through-thickness location. The left-hand side that was the maximum was then singled out. For all cylinders, the maximum left-hand side value was below unity, which implied that for an internal pressure of 100 psi failure had not yet occurred. An internal pressure at which each cylinder would begin to fail, or the failure pressure, was predicted by linearly extrapolating, namely, multiplying the maximum left-hand side of the equation by a variable p_f, such that,

$$(LHS_{\max})p_f = 1 \ . \tag{6.1}$$

It follows, then, that the failure pressure was given by

$$p_f = \frac{1}{LHS_{\max}} p_o , \tag{6.2}$$

where p_o is 100 psi. The particular left-hand side which was maximum identified the failure mode.

For the Hashin criterion, the four left-hand sides in the criterion were computed as a function of axial, circumferential, and through-thickness location. The left-hand side that was the maximum was then singled out. Again, for all cylinders the maximum left-hand side value was below unity. For the tensile modes of failure, the failure pressure was predicted by linearly extrapolating, namely, multiplying the maximum left-hand side of the equation by the square of a variable p_f, such that,

$$(LHS_{\max}) p_f^2 = 1 . \tag{6.3}$$

It follows, then, that the failure pressure was given by

$$p_f = \sqrt{\frac{1}{LHS_{\max}}} p_o , \tag{6.4}$$

where p_o is 100 psi. In the case of compressive matrix failure, failure pressure was determined by eq. 6.4 if $\left[\left(\frac{\sigma_T^-}{2\tau_T}\right)^2 - 1\right] = 0$. If $\left[\left(\frac{\sigma_T^-}{2\tau_T}\right)^2 - 1\right] \neq 0$, then the failure pressure was determined by

$$p_f = \left(\frac{-b \pm \sqrt{4a + b^2}}{2a}\right) p_o \tag{6.5}$$

where

$$\begin{aligned} a &= \left(\frac{\sigma_{22}}{2\tau_T}\right)^2 + \left(\frac{\sigma_{23}}{\tau_T}\right)^2 + \frac{1}{\tau_A^2}(\sigma_{12}^2 + \sigma_{13}^2) \\ b &= \frac{\sigma_{22}}{\sigma_T^-}\left[\left(\frac{\sigma_T^-}{2\tau_T}\right)^2 - 1\right]. \end{aligned} \tag{6.6}$$

For compressive fiber failure, eq. 6.2 was applied. The particular left-hand side which was maximum identified the failure mode.

Table 6-1 shows the failure pressure and location for axially-stiff, quasi-isotropic, circumferentially-stiff elliptical cylinders as predicted by the Hashin criterion. Recall, the axially-stiff and circumferentially-stiff cylinders are nine layers thick and have a total thickness of H=0.0495 in., and the quasi-isotropic cylinder is eight layers with a total thickness H=0.044 in. The location of failure through the thickness is specified both by indicating the value of the ζ coordinate, and by indicating the layer number and interface number for that layer. The footnote in the table explains the layer and interface numbering scheme. The circumferential location is denoted by the value of *s/C*. Also shown in table 6-1 are the values of the stress components at the location of failure when the pressure equals the failure pressure. Note that in each case failure occurs at the ends of the cylinders. This is due to effects associated with the clamped end conditions. It is important to realize that there are two ends of the cylinder and the *s/C* location noted is the crown location. There is a companion circumferential location in the keel where the failure conditions are satisfied at exactly the same pressure. As can be seen, in all cases σ_2 is generally close to the failure level of 7250 psi at the failure pressure (see eq. 5.1). In each case failure is attributed mainly to tension in the matrix, or σ_2. For the quasi-isotropic and axially-stiff laminates failure occurs at the inner radius and thus the interlaminar shear stresses do not contribute to failure of these cylinders. As failure occurs in layer seven of the circumferentially-stiff laminate, near the outer radius, the interlaminar shear stresses could contribute to the failure, but, in fact, are an order of magnitude less than inplane stress σ_2, and therefore have little bearing on the failure predictions. In general, the interlaminar shear stresses are always an order of magnitude less than the inplane stresses. Therefore, the interlaminar shear stresses can be computed from the geometri-

cally linear equilibrium equations, as has been done in the preceding sections, with little effect on the failure predictions for the geometrically nonlinear theory. Note that for the circumferentially-stiff laminate failure occurs exactly at the two side locations, $s/C=\pm 0.25$, simultaneously.

Table 6-1. Failure pressure and location for elliptical graphite-epoxy cylinders, geometrically linear analysis, Hashin failure criterion

	p_f (psi)	*loc**	ζ	*s/C***	σ_1 (psi)	σ_2 (psi)	τ_{12} (psi)	τ_{13} (psi)	τ_{23} (psi)
Axially-stiff	130.4	1/1 (+45)	-0.0248	-0.07	16200	6980	-3950	0	0
Quasi-isotropic	130.9	1/1 (+45)	-0.0220	-0.07	13200	6990	-3880	0	0
Circumferentially-stiff	106.7	7/2 (90)	0.0138	±0.25	2180	7250	-4.28	82.5	-663

* Location is given as layer number/interface, where 1 is the innermost layer and 1 denotes the inner and 2 the outer interface. The fiber direction of the layer is shown in parenthesis.
** All failures occur at the ends of the cylinders: $s/C=0$ is crown, $s/C=\pm 0.25$ are sides, C=circumference, s=arclength measure (see fig. 1-2)

As a comparison to the Hashin criterion, table 6-2 shows the failure pressure and location for the three elliptical cylinders as predicted by the maximum stress criterion. Again the failure mode is predicted to be due to σ_2 at the ends of the cylinders. The table shows the values of the stresses at the location of failure when the pressure equals the failure pressure. Note that σ_2 equals its failure value (see eq. 5.1). Any deviation from an exact σ_2=7250 psi is due to round off and other numerical anomalies that result from all the algorithms involved in the calculations. By comparing tables 6-1 and 6-2 it is seen that the Hashin and maximum stress criteria both predict similar scenarios, namely failure due to matrix cracking caused by high values of σ_2 at very similar, if not identical, locations.

Table 6-2. Failure pressure and location for elliptical graphite-epoxy cylinders, geometrically linear analysis, maximum stress failure criterion

	p_f (psi)	loc*	ζ	*s/C***	σ_1 (psi)	σ_2 (psi)	τ_{12} (psi)	τ_{13} (psi)	τ_{23} (psi)
Axially-stiff	135.6	1/1 (+45)	-0.0248	-0.07	16800	7260	-4110	0	0
Quasi-isotropic	135.6	1/1 (+45)	-0.0220	-0.08	6790	7260	-3840	0	0
Circumfer-entially-stiff	106.8	7/2 (90)	0.0138	±0.25	2180	7250	-4.28	82.6	-663

* Location is given as layer number/interface, where 1 is the innermost layer and 1 denotes the inner and 2 the outer interface. The fiber direction of the layer is shown in parenthesis.
** All failures occur at the ends of the cylinders: *s/C*=0 is crown, *s/C*=±0.25 are sides, *C*=circumference, *s*=arclength measure (see fig. 1-2)

Since all the failures in table 6-1 and 6-2 are matrix cracking failures, these can be considered first ply, or initial, failures. Catastrophic failure of the cylinder is not expected. Increased pressure capacity beyond the pressure levels in the tables is highly likely. However, when fibers begin to fail, failure of the cylinder is more likely. Failure of fibers in tension will lead to increased tension in the surrounding fibers. Failure of fibers in compression could lead to crushing and deterioration of the material in the surrounding region. For either situation, there could be a sudden cascading effect which would lead to catastrophic failure. Because of this, the pressures required to produce first fiber failure were computed. Table 6-3 and 6-4 show these pressures. These pressures were computed by ignoring all failures except fiber failure. For the Hashin criterion, this means either eq. 5.12 or 5.13 governs failure, while for the maximum stress criterion, this means the first of either eq. 5.5 or 5.6 governs. First fiber failures are predicted to be fiber compression failure in all cases. The location is again at the ends of the cylinders. Fiber crushing is predicted to occur at the outer radius, due to high bending effects. The predicted fiber failure

pressures are about twice as high as the predicted matrix cracking pressures. The Hashin and maximum stress criteria predict identical results because for the fiber compression failure mode, the Hashin criterion (eq. 5.13) and the maximum stress condition (the first of eq. 5.6) are identical equations. It is interesting to note that at the locations where the fibers fail by compression, the matrix is also in compression and near or beyond its failure level and the shear stress τ_{12} is more than one-half its failure level. Interlaminar stress does not play a role because of their small magnitudes.

A comment is in order regarding failure due to internal pressure. By the nature of pressure, a matrix crack in the inner layer will allow the pressure to reach the faces of the crack and perhaps force them apart further than if, for example, a bladder was used inside the cylinder to contain the pressure. In fact with a crack in the first layer and no bladder, the pressure reaches the second layer from within. This pressure could act to separate the second layer from the inner layer. With a bladder this would not happen, since the mechanics of force equilibrium around the crack would be different with a bladder, the bladder still reacting to the pressure force despite the matrix crack. It is not clear what the first matrix crack means in the presence of a bladder when compared to the case of no bladder. It is felt that with no bladder the first matrix crack has the potential for triggering failure, whereas with a bladder it is felt the first matrix crack could well be inconsequential.

Table 6-3. First fiber failure pressure and location for elliptical graphite-epoxy cylinders, geometrically linear analysis, Hashin failure criterion

	p_f (psi)	loc*	ζ	*s/C***	σ_1 (psi)	σ_2 (psi)	τ_{12} (psi)	τ_{13} (psi)	τ_{23} (psi)
Axially-stiff	242.1	9/2 (+45)	0.0248	-0.08	-180000	-5860	7800	-91.0	81.3
Quasi-isotropic	228.8	8/2 (+45)	0.0220	-0.07	-180000	-7070	8400	-112	95.9
Circumfer-entially-stiff	227.5	9/2 (+45)	0.0248	-0.06	-180000	-8710	9240	-109	91.7

* Location is given as layer number/interface, where 1 is the innermost layer and 1 denotes the inner and 2 the outer interface. The fiber direction of the layer is shown in parenthesis.
** All failures occur at the ends of the cylinders: *s/C*=0 is crown, *s/C*=±0.25 are sides, *C*=circumference, *s*=arclength measure (see fig. 1-2)

Table 6-4. First fiber failure pressure and location for elliptical graphite-epoxy cylinders, geometrically linear analysis, maximum stress failure criterion

	p_f (psi)	loc*	ζ	*s/C***	σ_1 (psi)	σ_2 (psi)	τ_{12} (psi)	τ_{13} (psi)	τ_{23} (psi)
Axially-stiff	242.1	9/2 (+45)	0.0248	-0.08	-180000	-5860	7800	-91.0	81.3
Quasi-isotropic	228.8	8/2 (+45)	0.0220	-0.07	-180000	-7070	8400	-112	95.9
Circumfer-entially-stiff	227.5	9/2 (+45)	0.0248	-0.06	-180000	-8710	9240	-109	91.7

* Location is given as layer number/interface, where 1 is the innermost layer and 1 denotes the inner and 2 the outer interface. The fiber direction of the layer is shown in parenthesis.
** All failures occur at the ends of the cylinders: *s/C*=0 is crown, *s/C*=±0.25 are sides, *C*=circumference, *s*=arclength measure (see fig. 1-2)

It was seen in chapter 3 that geometric nonlinearities have an influence on the response of elliptical cylinders subjected to internal pressure. An important issue is how the inclusion of geo-

metric nonlinearities influences the predictions of failure. To that end, the next section addresses the prediction of failure when geometrically nonlinear analyses are used.

6.2 Failure Predictions from the Geometrically Nonlinear Theory

To compute the failure pressure using the geometrically nonlinear analysis, iteration must be used, each iteration using a different internal pressure. The first step in the iteration process follows the failure analysis for the geometrically linear case, namely, the analysis is conducted for a pressure of p_o=100 psi. Then, considering the maximum stress criterion as an example, the seven left-hand sides of the failure criterion are computed, and using p_o=100 psi the failure pressure is computed using eq. 6.2. The geometrically nonlinear analysis is then conducted using this predicted failure pressure, i.e., now p_o is the failure pressure predicted from the first step. The seven left-hand sides are again computed and eq. 6.2 is used to compute a new failure pressure. If this failure pressure prediction is within 10% of the first iteration's failure pressure prediction, the iteration process is considered converged. If the second failure pressure prediction is not with 10% of the first prediction, the geometrically nonlinear analysis is repeated using the second failure pressure prediction as p_o and the failure predictions made again using eq. 6.2. A similar iteration procedure is used for the Hashin criterion based on eq. 6.2, 6.4, or 6.5 and the four left-hand sides in that criterion.

Tables 6-5 through 6-8 represent the geometrically nonlinear case counterpart to tables 6-1 through 6-4, which were computed using geometrically linear analysis. Table 6-5 shows the failure pressure and location for axially-stiff, quasi-isotropic, and circumferentially-stiff elliptical cylinders as predicted by the Hashin failure criterion. Also shown are the values of the stress components at the location of failure when the pressure equals the failure pressure. Note that in each

case failure occurs at the ends of the cylinders. As can be seen, in all cases σ_2 is generally near the failure level of 7250 psi at the failure pressure and, therefore, in each case failure is attributed mainly to tension in the matrix, or σ_2. For the quasi-isotropic and axially-stiff laminates failure occurs at the inner radius and thus again the interlaminar shear stresses do not contribute to this failure of the cylinder. As failure occurs in layer seven of the circumferentially-stiff laminate, near the outer radius, the interlaminar shear stresses could contribute to the initial failure, but, in fact, are an order of magnitude less than inplane stress σ_2, and therefore again have little bearing on the failure predictions. Comparing tables 6-1 and 6-5, it is seen than nonlinearities are predicted to have minimal influence on the failure predictions. The failure pressure levels for the axially-stiff and quasi-isotropic cylinders are predicted to be slightly greater for the nonlinear analysis, and the *s/C* locations of failure are predicted to be somewhat farther away from the crown, i.e., the *s/C*=0 location. On the other hand, compared to the geometrically linear case, the geometrically nonlinear analysis for the circumferentially-stiff case predicts a slightly lower failure pressure but the same *s/C* location.

Table 6-5. Failure pressure and location for elliptical graphite-epoxy cylinders, geometrically nonlinear analysis, Hashin failure criterion

	p_f (psi)	*loc**	ζ	*s/C***	σ_1 (psi)	σ_2 (psi)	τ_{12} (psi)	τ_{13} (psi)	τ_{23} (psi)
Axially-stiff	135.3	1/1 (+45)	-0.0248	-0.09	13100	6990	-3870	0	0
Quasi-isotropic	134.1	1/1 (+45)	-0.0220	-0.10	4540	7020	-3650	0	0
Circumfer-entially-stiff	104.9	7/2 (+90)	0.0138	±0.25	2170	7230	-6.04	105	-803

* Location is given as layer number/interface, where 1 is the innermost layer and 1 denotes the inner and 2 the outer interface. The fiber direction of the layer is shown in parenthesis.
** All failures occur at the ends of the cylinders: *s/C*=0 is crown, *s/C*=±0.25 are sides, *C*=circumference, *s*=arclength measure (see fig. 1-2)

As a comparison to the Hashin criterion, table 6-6 shows the failure pressure and location for the three elliptical cylinders as predicted by the maximum stress criterion and the geometrically nonlinear analysis. Again the failure mode is predicted to be due to σ_2 at the ends of the cylinders. The table shows the values of the stresses at the location of failure when the pressure equals the failure pressure. Note that σ_2 equals its failure value. By comparing tables 6-5 and 6-6 it is seen that the Hashin and maximum stress criteria both predict similar scenarios, namely failure due to matrix cracking caused by high values of σ_2 at very similar, in not identical, locations. Furthermore, by comparing tables 6-2 and 6-6, it is seen that according to the maximum stress criterion, geometric nonlinearities predict slightly increased failure pressures for the axially-stiff and quasi-isotropic cases, with the failures occurring somewhat farther away from the *s/C*=0 location. For the circumferentially-stiff case, the nonlinear analysis predicts the same *s/C* location and a slightly lower failure pressure. This relationship between linear and nonlinear analyses for the

maximum stress criterion is identical to the relationship between linear and nonlinear analyses for the Hashin criterion.

Table 6-6. Failure pressure and location for elliptical graphite-epoxy cylinders, geometrically nonlinear analysis, maximum stress failure criterion

	p_f (psi)	loc*	ζ	*s/C***	σ_1 (psi)	σ_2 (psi)	τ_{12} (psi)	τ_{13} (psi)	τ_{23} (psi)
Axially-stiff	140.3	1/1 (+45)	-0.0248	-0.10	7990	7250	-3860	0	0
Quasi-isotropic	138.6	1/1 (+45)	-0.0220	-0.10	4700	7250	-3780	0	0
Circumfer-entially-stiff	105.0	7/2 (90)	0.0138	±0.25	2170	7250	-6.05	105	-804

* Location is given as layer number/interface, where 1 is the innermost layer and 1 denotes the inner and 2 the outer interface. The fiber direction of the layer is shown in parenthesis.
** All failures occur at the ends of the cylinders: *s/C*=0 is crown, *s/C*=±0.25 are sides, *C*=circumference, *s*=arclength measure (see fig. 1-2)

The pressure required to produce first fiber failure for the geometrically nonlinear cases are shown in tables 6-7 and 6-8. Using the Hashin failure criterion, first fiber failures are predicted to be fiber compression failure in all cases except for the circumferentially-stiff laminate. The location is again at the ends of the cylinders. Except for the circumferentially-stiff laminate, failure is predicted to occur at the outer radius, again due to high bending effects. Note that for these two cases of high fiber compressive stresses, the matrix is in a high compressive state and the shear stress τ_{12} is about one-half its failure level. Also for these two cases, compared to the geometrically linear case of table 6-3, geometric nonlinearities lead to somewhat higher first fiber failure pressures, and failure locations further away from *s/C*=0. The failure pressures for these two first fiber failure cases are about a factor of two greater than the matrix failure pressures of table 6-5, as in the linear case.

The prediction for the first fiber failure for the circumferentially-stiff case in table 6-7 is quite interesting. The Hashin criterion and the nonlinear analysis predict first fiber failure to be tensile in the outer layer at the sides of the cylinder, whereas, according to table 6-3, the linear analysis predicted fiber compressive failure in the outer layer at the crown of the cylinder. For the nonlinear analysis of table 6-7, both σ_2 and τ_{12} are larger in magnitude than in table 6-3. Since the Hashin criterion uses a combination of stresses, it appears that the high tensile σ_1 and high values of σ_2 and τ_{12} for the geometrically nonlinear case combine to produce fiber tensile failure as opposed to fiber compressive failure, and the location of failure is different. If the variation of curvature with circumferential location at the end of the cylinder, particularly the sign change from side to crown (see fig. A-15) is examined, it can be seen why the failure in the outer layer could be tensile in the cylinder sides or compressive in the crown. For the circumferentially-stiff geometrically nonlinear case, in addition to the failure mode changing relative to the linear case, the failure pressure is higher. Also, the first fiber failure pressure predicted by the nonlinear analysis is, as has been the case, about a factor of two greater than for the first matrix failure predicted by the nonlinear analysis.

Table 6-7. First Fiber failure pressure and location for elliptical graphite-epoxy cylinders, geometrically nonlinear analysis, Hashin failure criterion

	p_f (psi)	loc*	ζ	*s/C***	σ_1 (psi)	σ_2 (psi)	τ_{12} (psi)	τ_{13} (psi)	τ_{23} (psi)
Axially-stiff	269.8	9/2 (+45)	0.0248	-0.11	-180000	-5070	7400	-1590	1580
Quasi-isotropic	260.6	8/2 (+45)	0.0220	-0.10	-180000	-5600	7660	-1460	1460
Circumfer-entially-stiff	248.0	9/2 (+45)	0.0248	0.24	153000	12100	-10187	-84.9	117

* Location is given as layer number/interface, where 1 is the innermost layer and 1 denotes the inner and 2 the outer interface. The fiber direction of the layer is shown in parenthesis.
** All failures occur at the ends of the cylinders: *s/C*=0 is crown, *s/C*=±0.25 are sides, *C*=circumference, *s*=arclength measure (see fig. 1-2)

As seen in table 6-8, the geometrically nonlinear analysis and the maximum stress criterion predict first fiber failure to be compressive for all three laminates. Compared to the analog geometrically linear analysis, table 6-4, the predicted failure locations are further away from the *s/C*=0 location and the pressure levels are higher. Also compared to the geometrically nonlinear maximum stress criterion analysis for matrix failure, table 6-6, the first fiber failure pressure for the axially-stiff and quasi-isotropic laminates are about factor of two higher, for the circumferentially-stiff laminate, the factor is about 2.5.

Table 6-8. First Fiber failure pressure and location for elliptical graphite-epoxy cylinders, geometrically nonlinear analysis, maximum stress failure criterion

	p_f (psi)	loc*	ζ	*s/C***	σ_1 (psi)	σ_2 (psi)	τ_{12} (psi)	τ_{13} (psi)	τ_{23} (psi)
Axially-stiff	269.8	9/2 (+45)	0.0248	-0.11	-180000	-5070	7400	-1590	1580
Quasi-isotropic	260.6	8/2 (+45)	0.0220	-0.10	-180000	-5600	7660	-1460	1460
Circumfer-entially-stiff	266.0	9/2 (+45)	0.0248	-0.09	-180000	-6380	8060	-877	865

* Location is given as layer number/interface, where 1 is the innermost layer and 1 denotes the inner and 2 the outer interface. The fiber direction of the layer is shown in parenthesis.
** All failures occur at the ends of the cylinders: *s/C*=0 is crown, *s/C*=±0.25 are sides, *C*=circumference, *s*=arclength measure (see fig. 1-2)

Tables 6-9 and 6-10 summarize the key results just discussed. Table 6-9 shows the failure pressure, location, and mode of failure for both the Hashin and maximum stress failure criteria for the cylinders. Results for both linear and nonlinear analysis have been included. As has been discussed, the differences in failure pressure and location of failure between linear and nonlinear analysis are quite small. In each case failure is due to tension in the matrix. In a general sense, both the axially-stiff and quasi-isotropic laminates are predicted to experience the first matrix crack at around 130-140 psi in the first layer (a +45° layer) at the inner radial location at s/C ≈ -0.10. The circumferentially-stiff laminate is predicted to experience the first matrix crack at around 105 psi in the seventh layer (a 90° layer) at the outer radial location at s/C = ±0.25. Whether failure is due to bending or inplane effect is examined by evaluating the part of the stress that is contributed by bending effects and comparing it with the part contributed by inplane effects. The ratio $\sigma_\kappa/\sigma_\varepsilon$ is the ratio of these two parts and the table shows that both the axially-stiff and the quasi-isotropic laminates are predicted to fail due to bending effects. On the other hand,

the circumferentially-stiff laminate is predicted to fail due to inplane effects. The bending effects at the end are induced by the conditions of w=0 and $\frac{\partial w}{\partial x}$ =0 there, while inplane effects are induced by the condition v=0 there and the inplane stress resultants caused by the internal pressure. Note that for the axially-stiff and quasi-isotropic cases, geometric nonlinearities reduce bending effects relative to inplane effects, whereas for the circumferentially-stiff case the reverse is true.

Table 6-9. Failure pressure, location, and mode for elliptical graphite-epoxy cylinders, geometrically linear and nonlinear analyses, two failure criteria

		Axially-Stiff		Quasi-Isotropic		Circumferentially-Stiff	
		Hashin	Max σ	Hashin	Max σ	Hashin	Max σ
linear	p_f, psi	130	136	131	136	107	107
	loc*	1/1 (+45)	1/1 (+45)	1/1 (+45)	1/1 (+45)	7/2 (90)	7/2 (90)
	ζ	-0.0248	-0.0248	-0.0220	-0.0220	0.0138	0.0138
	s/C**	-0.07	-0.07	-0.07	-0.08	±0.25	±0.25
	mode $\sigma_\kappa/\sigma_\varepsilon$	$+\sigma_2$ 3.3/1	$+\sigma_2$ 3.3/1	$+\sigma_2$ 4/1	$+\sigma_2$ 2.86/1	$+\sigma_2$ 0.33/1	$+\sigma_2$ 0.33/1
nonlinear	p_f, psi	135	140	134	139	105	105
	loc	1/1 (+45)	1/1 (+45)	1/1 (+45)	1/1 (+45)	7/2 (90)	7/2 (90)
	ζ	-0.0248	-0.0248	-0.0220	-0.0220	0.0138	0.0138
	s/C**	-0.09	-0.10	-0.10	-0.10	±0.25	±0.25
	mode $\sigma_\kappa/\sigma_\varepsilon$	$+\sigma_2$ 2.7/1	$+\sigma_2$ 2.3/1	$+\sigma_2$ 2.2/1	$+\sigma_2$ 2.2/1	$+\sigma_2$ 0.38/1	$+\sigma_2$ 0.38/1

* Location is given as layer number/interface, where 1 is the innermost layer and 1 denotes the inner and 2 the outer interface. The fiber direction of the layer is shown in parenthesis.
** All failures occur at the ends of the cylinders: s/C=0 is crown, s/C=±0.25 are sides, C=circumference, s=arclength measure (see fig. 1-2)

Table 6-10 shows the failure pressure and location of failure for the Hashin failure criterion and examines matrix (as seen in table 6-9) and fiber failure. Results for both linear and nonlinear analysis have been included. The most notable difference between first fiber and matrix failure is the increase in failure pressure from 105-135 psi to 227-270 psi. This indicates that as the pressure increases the matrix will fail long before the first fiber failure pressure is reached. Also, from matrix failure to first fiber failure, the location of failure shifts dramatically from the inside to the outside of the cylinder for the axially-stiff and quasi-isotropic laminates, and from the outer 90° layer to the outer +45° layer for the circumferentially-stiff laminate. Geometric nonlinearities have a somewhat stronger influence on first fiber failure pressure as compared to matrix failure, causing increases in failure pressure around 10%, as opposed to 2% for matrix failure pressures. Based on the nonlinear analysis, the axially-stiff laminate fibers fail at 270 psi in the ninth layer, the outer +45° layer, on the outer interface at s/C = -0.11. The quasi-isotropic laminate fibers fail at 261 psi in the eighth layer, the outer +45° layer, on the outer interface at s/C = -0.10. The circumferentially-stiff laminate fibers fail at 248 psi in the ninth layer, the outer +45° layer, on the outer interface at s/C = 0.24.

Table 6-10. Failure pressure, location, and mode for elliptical graphite-epoxy cylinders, geometrically linear and nonlinear analyses, two failure modes, Hashin failure criterion

		Axially-Stiff		Quasi-Isotropic		Circumferentially-Stiff	
		Matrix	Fiber	Matrix	Fiber	Matrix	Fiber
linear	p_f, psi	130	242	131	229	107	227
	loc*	1/1 (+45)	9/2 (+45)	1/1 (+45)	8/2 (+45)	7/2 (90)	9/2 (+45)
	ζ	-0.0248	0.0248	-0.0220	0.0220	0.0138	0.0248
	*s/C***	-0.07	-0.08	-0.07	-0.07	±0.25	-0.06
	mode $\sigma_\kappa/\sigma_\varepsilon$	$+\sigma_2$ 3.3/1	$-\sigma_1$ 1.25/1	$+\sigma_2$ 4/1	$-\sigma_1$ 1.3/1	$+\sigma_2$ 0.33/1	$-\sigma_1$ 1.25/1
nonlinear	p_f, psi	135	270	134	261	105	248
	loc*	1/1 (+45)	9/2 (+45)	1/1 (+45)	8/2 (+45)	7/2 (90)	9/2 (+45)
	ζ	-0.0248	0.0248	-0.0220	0.0220	0.0138	0.0248
	*s/C***	-0.09	-0.11	-0.10	-0.10	±0.25	0.24
	mode $\sigma_\kappa/\sigma_\varepsilon$	$+\sigma_2$ 2.7/1	$-\sigma_1$ 1.2/1	$+\sigma_2$ 2.2/1	$-\sigma_1$ 1.2/1	$+\sigma_2$ 0.38/1	$+\sigma_1$ 0.59/1

* Location is given as layer number/interface, where 1 is the innermost layer and 1 denotes the inner and 2 the outer interface. The fiber direction of the layer is shown in parenthesis.
** All failures occur at the ends of the cylinders: *s/C*=0 is crown, *s/C*=±0.25 are sides, *C*=circumference, *s*=arclength measure (see fig. 1-2)

6.3 An Alternative View of Failure Predictions

With composite materials there is often scatter in the results of tests designed to determine failure stresses. Considering the failure stress of a composite material to be exactly a certain level is somewhat unrealistic. The scatter is due to small unpredictable irregularities in the microstructure of composites and possible anomalies in the manufacturing process. As a result, the location with the highest stress may not fail first. A slightly lower stress at another location, coupled with a microstructural irregularity, could lead to lower failure stress levels. To that end, the geometri-

cally nonlinear failure analysis was used to compute the locations within the ellipse where the seven left-hand sides in the Hashin failure criterion were within 20% of the failure level, i.e., the left-hand sides were in the range 0.80 to 1.00, with 1.00 corresponding to the cases discussed in table 6-5.

Figures 6-1 through 6-3 show the locations of the maximum left-hand side and all values within 20% of the maximum value for the Hashin failure criterion for the axially-stiff, quasi-isotropic, and circumferentially-stiff laminates. The axially-stiff, quasi-isotropic, and circumferentially-stiff laminates were evaluated using nonlinear analysis at failure pressure, p_f. In each figure a greatly distorted view of the crown section of the cylinder wall through the thickness from $-H/2 \le \zeta \le H/2$, around the circumference from $-0.25 \le s/C \le 0.25$, and at $x/L=0.5$ provides a visual display of the points within 20% of failure. Each figure includes a table which lists in descending order the location of the points, and stresses at those points at the failure pressure.

Figure 6-1 shows all points within 20% of the maximum left-hand side value for the axially-stiff laminate, which has a thickness, H, of 0.0495 in. As indicated in previous tables, the maximum left-hand side value, or initial failure point, is located at the first layer, a +45° layer, at the inner radial location of the cylinder at $s/C=-0.09$. Considering points where the left-hand side is less than 1.00, the points are dispersed circumferentially on both sides of the initial failure point, but remain in the first layer at the inner radial location. Eventually, the points reach to both sides of the interface between the first and second layers. An alternative interpretation of the spatial distribution of the points is that if the pressure is increased beyond the value to predict failure at point 1, point 2 will be the next location of failure. Further increases in pressure would lead to failure at points 3, 4, 5, etc. With this interpretation, then, it is felt that the geometric distribution of points would represent the progression of damage as the pressure increases beyond the value

necessary to have the Hashin criteria to equal 1.00. If this is the case, then, matrix cracking will accumulate in layer 1 at the inner radial location (ζ=-0.02475) in the range $-0.16 \le s/C \le 0$. There will also be cracking in layer 2 at the interface between the 1st and 2nd layers (ζ=-0.01925). All these failures would be due to high values of σ_2.

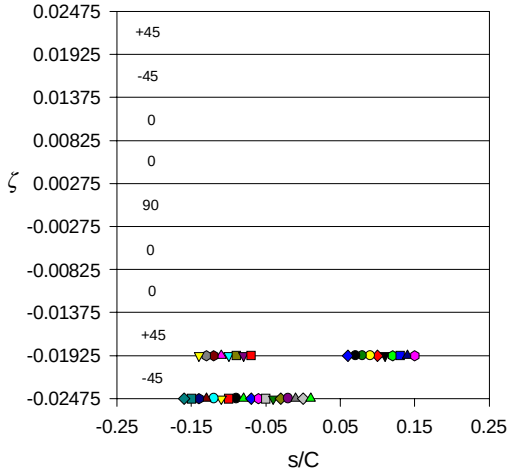

	loc	ζ	*s/C*	σ_1	σ_2	τ_{12}	τ_{13}	τ_{23}
1	1/1 (+45)	-0.02475	-0.090	13100	6990	-3870	0	0
2	1/1 (+45)	-0.02475	-0.100	7700	6990	-3730	0	0
3	1/1 (+45)	-0.02475	-0.080	18500	6950	-4000	0	0
4	1/1 (+45)	-0.02475	-0.110	2430	6950	-3570	0	0
5	1/1 (+45)	-0.02475	-0.070	23900	6870	-4110	0	0
6	1/1 (+45)	-0.02475	-0.060	29300	6770	-4200	0	0
7	1/1 (+45)	-0.02475	-0.120	-2710	6860	-3380	0	0
8	1/1 (+45)	-0.02475	-0.050	34700	6640	-4280	0	0
9	1/1 (+45)	-0.02475	-0.130	-7590	6710	-3170	0	0
10	1/1 (+45)	-0.02475	-0.040	39900	6490	-4340	0	0
11	1/1 (+45)	-0.02475	-0.030	45100	6320	-4390	0	0
12	1/1 (+45)	-0.02475	-0.140	-12100	6490	-2950	0	0
13	1/1 (+45)	-0.02475	-0.020	50100	6120	-4430	0	0
14	1/1 (+45)	-0.02475	-0.150	-16100	6220	-2700	0	0
15	1/1 (+45)	-0.02475	-0.010	54900	5900	-4450	0	0
16	2/1 (-45)	-0.01925	0.110	-7030	6050	2850	-133	-775
17	2/1 (-45)	-0.01925	0.100	-2500	6020	2960	-135	-812

Figure 6-1. Points within 20% of failure pressure, Hashin criterion, axially-stiff laminate, nonlinear analysis, x/L=0.5

18	2/1 (-45)	-0.01925	0.120	-11300	6040	2740	-132	-728
19	2/1 (-45)	-0.01925	0.090	2210	5940	3050	-135	-841
20	2/1 (-45)	-0.01925	0.130	-15300	5980	2600	-129	-671
21	1/2 (+45)	-0.01925	-0.110	-8310	5930	-2770	-954	119
22	1/2 (+45)	-0.01925	-0.100	-3660	5910	-2880	-966	122
23	1/1 (+45)	-0.02475	0.000	59600	5670	-4460	0	0
24	1/2 (+45)	-0.01925	-0.120	-12700	5910	-2630	-938	113
25	2/1 (-45)	-0.01925	0.080	7050	5850	3130	-136	-865
26	1/2 (+45)	-0.01925	-0.090	1180	5860	-2990	-972	125
27	2/1 (-45)	-0.01925	0.140	-18700	5870	2460	-124	-599
28	1/2 (+45)	-0.01925	-0.080	6140	5780	-3070	-975	127
29	1/1 (+45)	-0.02475	-0.160	-19600	5870	-2440	0	0
30	1/2 (+45)	-0.01925	-0.130	-16800	5840	-2490	-911	107
31	2/1 (-45)	-0.01925	0.070	12000	5720	3210	-136	-883
32	1/2 (+45)	-0.01925	-0.070	11100	5660	-3150	-976	129
33	1/1 (+45)	-0.02475	0.010	64200	5420	-4460	0	0
34	1/2 (+45)	-0.01925	-0.140	-20300	5720	-2330	-871	100
35	2/1 (-45)	-0.01925	0.060	17000	5580	3270	-136	-899
36	2/1 (-45)	-0.01925	0.150	-21600	5700	2290	-118	-514

Figure 6-1. Points within 20% of failure pressure, Hashin criterion, axially-stiff laminate, nonlinear analysis, x/L=0.5

Figure 6-2 shows all points within 20% of the maximum left-hand side value for the quasi-isotropic laminate, which has a thickness, *H*, of 0.044 in. As indicated in previous tables, the initial failure point is located in the first layer at the inner radial location of the cylinder at *s/C*=-0.100. Considering points where the left-hand side is less than 1.00, the points are dispersed circumferentially on both sides of the initial failure point but remain in the first layer at the inner radial location. Eventually the points reach to both sides of the interface between the first and second layers, and the outer radial location of the eighth layer. An alternative interpretation of the spatial distribution of the points is that matrix cracking will accumulate in layer 1 at the inner radial location (ζ=-0.02220) in the range $-0.16 \le s/C \le 0$. There will also be cracking in layers 1 and 2 at the interface between these layers (ζ=-0.0165). Some cracking will also occur in layer 8 at the outer location (ζ=0.0220). All these failures would be due to high values of σ_2.

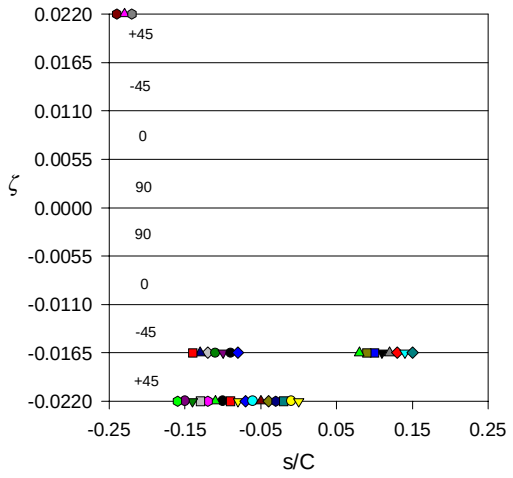

	loc	ζ	*s/C*	σ_1	σ_2	τ_{12}	τ_{13}	τ_{23}
1	1/1 (+45)	-0.0220	-0.100	4540	7020	-3650	0	0
2	1/1 (+45)	-0.0220	-0.090	9800	7000	-3790	0	0
3	1/1 (+45)	-0.0220	-0.110	-567	7000	-3510	0	0
4	1/1 (+45)	-0.0220	-0.080	15200	6930	-3900	0	0
5	1/1 (+45)	-0.0220	-0.120	-5470	6910	-3330	0	0
6	1/1 (+45)	-0.0220	-0.070	20500	6830	-3990	0	0
7	1/1 (+45)	-0.0220	-0.060	26000	6710	-4080	0	0
8	1/1 (+45)	-0.0220	-0.130	-10100	6780	-3150	0	0
9	1/1 (+45)	-0.0220	-0.050	31500	6550	-4150	0	0
10	1/1 (+45)	-0.0220	-0.140	-14200	6580	-2930	0	0
11	1/1 (+45)	-0.0220	-0.040	36800	6380	-4200	0	0
12	1/1 (+45)	-0.0220	-0.030	42200	6180	-4250	0	0
13	1/1 (+45)	-0.0220	-0.150	-17900	6330	-2700	0	0
14	1/1 (+45)	-0.0220	-0.020	47500	5970	-4280	0	0
15	2/1 (-45)	-0.0165	0.120	-14800	6040	2640	-154	-844
16	2/1 (-45)	-0.0165	0.110	-10900	6010	2740	-157	-902
17	2/1 (-45)	-0.0165	0.130	-18200	6020	2550	-150	-771
18	1/1 (+45)	-0.0220	-0.160	-20700	6000	-2470	0	0
19	1/1 (+45)	-0.0220	-0.010	52600	5730	-4300	0	0
20	2/1 (-45)	-0.0165	0.100	-6760	5930	2810	-159	-946
21	8/2 (+45)	0.0220	-0.230	32100	5810	-3790	-14.6	-3.36
22	2/1 (-45)	-0.0165	0.140	-21100	5960	2440	-142	-679
23	1/2 (+45)	-0.0165	-0.120	-16400	5870	-2520	-1060	130
24	8/2 (+45)	0.0220	-0.240	45000	5680	-4080	-15.4	6.02
25	1/2 (+45)	-0.0165	-0.110	-12500	5860	-2620	-1090	136

Figure 6-2. Points within 20% of failure pressure, Hashin criterion, quasi-isotropic laminate, nonlinear analysis, x/L=0.5

26	2/1 (-45)	-0.0165	0.090	-2340	5830	2870	-159	-980
27	1/2 (+45)	-0.0165	-0.130	-19900	5850	-2410	-1020	121
28	1/2 (+45)	-0.0165	-0.100	-8190	5810	-2700	-1100	141
29	2/1 (-45)	-0.0165	0.150	-23200	5830	2310	-132	-567
30	8/2 (+45)	0.0220	-0.220	17400	5680	-3330	-11.5	-12.6
31	1/2 (+45)	-0.0165	-0.090	-3630	5720	-2790	-1120	144
32	1/2 (+45)	-0.0165	-0.140	-22900	5770	-2290	-964	109
33	2/1 (-45)	-0.0165	0.080	2290	5700	2930	-159	-1010
34	1/1 (+45)	-0.0220	0.000	57600	5480	-4310	0	0
35	1/2 (+45)	-0.0165	-0.080	1150	5600	-2850	-1120	148

Figure 6-2. Points within 20% of failure pressure, Hashin criterion, quasi-isotropic laminate, nonlinear analysis, x/L=0.5

Figure 6-3 shows all points within 20% of the maximum left-hand side value for the circumferentially-stiff laminate, which has a thickness, *H*, of 0.0495 in. As indicated in previous tables, the initial failure points are located at the outer interface in the seventh layer, a 90° layer, at *s/C*=±0.25. Considering points where the left-hand side is less than 1.00, the points are located at the outer interface of the seventh layer and inward of *s/C*=±0.25. The points are also located at the inner and outer interfaces of other layers, and inward of *s/C*=±0.25. An alternative interpretation of the spatial distribution of the points is that as pressure increases matrix cracking will accumulate in layer 7 at the outer interface location (ζ=0.01375) in the ranges $-0.25 \le s/C \le -0.22$ and $0.22 \le s/C \le 0.25$. There will also be cracking in layer 6 at the interface between layers 6 and 7 (ζ=0.00825). Some cracking will also occur in layer 8 at the interface between layers 8 and 9 (ζ=0.01925), and at the outer radial location in layer 9 (ζ=0.02475). All these failures would be due to high values of σ_2.

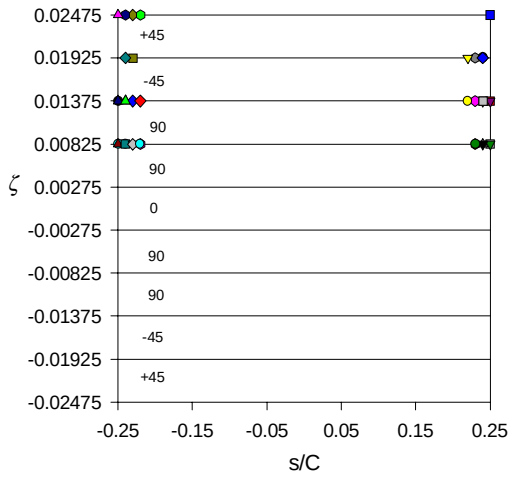

	loc	ζ	*s/C*	σ_1	σ_2	τ_{12}	τ_{13}	τ_{23}
1	7/2 (90)	0.01375	-0.250	2170	7230	-6.04	105	-803
2	7/2 (90)	0.01375	0.250	2170	7230	-6.04	105	-803
3	7/2 (90)	0.01375	-0.240	2140	7130	547	33.2	-783
4	7/2 (90)	0.01375	0.240	2130	7100	-559	169	-760
5	7/2 (90)	0.01375	-0.230	2030	6770	1080	-40.4	-702
6	7/2 (90)	0.01375	0.230	2010	6710	-1090	221	-658
7	6/2 (90)	0.00825	-0.250	1940	6450	-6.04	105	-866
8	6/2 (90)	0.00825	0.250	1940	6450	-6.04	105	-866
9	7/1 (90)	0.00825	-0.250	1940	6450	-6.04	105	-866
10	7/1 (90)	0.00825	0.250	1940	6450	-6.04	105	-866
11	9/2 (+45)	0.02475	-0.230	42300	6070	-4190	2.88	-22.6
12	9/2 (+45)	0.02475	-0.240	52400	6020	-4440	7.46	-17.8
13	6/2 (90)	0.00825	-0.240	1910	6350	547	31.9	-844
14	7/1 (90)	0.00825	-0.240	1910	6350	547	31.9	-844
15	6/2 (90)	0.00825	0.240	1900	6330	-559	171	-819
16	7/1 (90)	0.00825	0.240	1900	6330	-559	171	-819
17	7/2 (90)	0.01375	-0.220	1860	6200	1570	-111	-571
18	9/2 (+45)	0.02475	-0.220	30800	5900	-3810	-0.861	-26.0
19	7/2 (90)	0.01375	0.220	1830	6100	-1580	259	-508
20	9/2 (+45)	0.02475	-0.250	60500	5720	-4510	12.6	-12.2
21	9/2 (+45)	0.02475	0.250	60500	5720	-4510	12.6	-12.2
22	6/2 (90)	0.00825	-0.230	1810	6060	1080	-43.4	-759
23	7/1 (90)	0.00825	-0.230	1810	6060	1080	-43.4	-759
24	6/2 (90)	0.00825	0.230	1800	6020	-1090	225	-710
25	7/1 (90)	0.00825	0.230	1800	6020	-1090	225	-710

Figure 6-3. Points within 20% of failure pressure, Hashin criterion, circumferentially-stiff laminate, nonlinear analysis, x/L=0.5

26	9/1 (+45)	0.01925	-0.230	37400	5610	-3840	394	-124
27	7/2 (90)	0.01375	-0.250	4260	5920	-3.72	57.0	-433
28	7/2 (90)	0.01375	0.250	4260	5920	-3.72	57.0	-433
29	9/1 (+45)	0.01925	-0.240	47100	5510	-4050	495	-127
30	8/2 (-45)	0.01925	0.230	36700	5560	3780	87.8	550
31	8/2 (-45)	0.01925	0.240	46600	5480	4020	108	577
32	7/2 (90)	0.01375	0.240	4250	5830	-556	78.0	-415
33	7/2 (90)	0.01375	-0.240	4210	5830	548	32.5	-421

Figure 6-3. Points within 20% of failure pressure, Hashin criterion, circumferentially-stiff laminate, nonlinear analysis, x/L=0.5

This chapter has presented a comprehensive discussion of failure of internally pressurized elliptical cylinders. The Hashin and maximum stress failure criteria, geometrically linear and nonlinear analyses, and first matrix failure and first fiber failure were considered. Additionally, the concept of an accumulation of matrix cracks was introduced. It was shown that for the first matrix failure there was not much difference between the predictions of the two failure criteria or between linear and nonlinear analyses. However, the predicted pressure to cause first fiber failure was about a factor of two higher than the predicted pressure to cause matrix failure. Additionally, considering nonlinear analysis, the Hashin prediction of first fiber failure for the circumferentially-stiff laminate was quite different than the prediction of the maximum stress criterion. The mode and location differed significantly, and the pressure levels were somewhat different. The next chapter summarizes this entire study, presents conclusions, and provides ideas for future work.